COMPDYN 2011
3rd ECCOMAS Thematic Conference on
Computational Methods in Structural Dynamics and Earthquake Engineering
M. Papadrakakis, M. Fragiadakis, V. Plevris (eds.)
Corfu, Greece, 25–28 May 2011

ANALYTICAL DISPLACEMENT-BASED SEISMIC FRAGILITY ANALYSIS OF STONE MASONRY BUILDINGS

Ahmad Abo-El-Ezz[1], Marie-José Nollet[2], Miroslav Nastev[3]

[1] Department of Construction Engineering, École de technologie supérieure, University of Québec
Montréal, Canada
e-mail: ahmad.abo-el-ezz.1@ens.etsmtl.ca

[2] Department of Construction Engineering, École de technologie supérieure, University of Québec
Montréal, Canada
e-mail: Marie-Jose.Nollet@etsmtl.ca

[3] Geological Survey of Canada, Natural Resources Canada.
Québec City, Canada.
e-mail: Miroslav.Nastev@RNCan-NRCan.gc.ca

Keywords: Seismic Risk Assessment, Fragility Analysis, Stone Masonry.

Abstract. *In an effort to reduce seismic risks, the Geological Survey of Canada has recently taken important steps by initiating a project on quantitative assessment of earthquake related risks. One of the objectives of this project is to study the seismic vulnerability of historic stone masonry buildings generally known for their poor performance during strong ground motion. This paper focuses on the development of analytical displacement-based fragility curves reflecting the characteristics of existing stone masonry buildings in Canada. The fragility analysis provides the necessary link between the building damage and earthquake intensity in a probabilistic setting, where the extent of building damage is best correlated to the amount of induced building displacement. The old historic center of Quebec City was selected as a typical study area due to the concentration of stone masonry buildings, which combined to the high heritage value increases the potential consequences of failure. Comparison was made with similar fragility curves implicit in Hazus-MH and ELER seismic risk assessment tools. Differences have been observed between the three sets of fragility curves which may lead to significantly disparate damage estimates. This comparison shows the importance of the development of fragility curves specific to the generic construction characteristics in the study area and emphasizes the need of critical use of existing risk assessment tools and generated results.*

1 INTRODUCTION

Majority of existing historic buildings in old urban centers in Eastern Canada are stone masonry structures and represent un-measurable architectural and cultural heritage. Historic stone masonry buildings were built to resist gravity loads only and generally offer poor resistance to lateral seismic loads. Damage occurred to stone masonry buildings from past earthquakes is attributed to inadequate structural integrity due to the lack of connection between stone masonry structural walls and wooden floors and roofs; and to ensuing inadequate structural resistance, which results into typical shear cracking and disintegration of stone walls and partial or total collapse of buildings [1].

The high seismic risks related to stone masonry buildings are even more increased due to their location in densely populated urban centers in a way that the consequences of failure of these structures tend to be severe with regards to human casualties, heritage damage and economic losses [2]. Seismic risk assessment of historic stone masonry buildings is therefore the first necessary step in providing mitigation plans for seismic retrofit and preservation.

In an effort to reduce seismic risks, the Geological Survey of Canada has recently taken important steps by initiating a project on quantitative assessment of earthquake related risks. One of the objectives of this project is to study the seismic vulnerability of historic stone masonry buildings. The old historic center of Quebec City was selected as a typical study area.

Seismic risk is often considered as the convolution of seismic hazard (expected ground motion at given location), exposure (demographics, buildings, essential facilities, utilities, etc.), and vulnerability (response of structures to earthquake impacts, generally defined by expected degree of damage under different levels of seismic loading). These three components are integrated to determine direct and indirect physical damage and losses. Fragility analysis is the key component in performance based seismic risk assessment. It provides the link between the two other components of the seismic risk assessment process, inventory and seismic hazard.

The most widely used risk assessment tool in North America, Hazus-MH [3], seems to not adequately represent the response of stone masonry structures to earthquake loading. It considers only one structural class for unreinforced masonry buildings, URM, mainly covering brittle brick masonry structures. The European ELER tool [4] recognizes explicitly the stone masonry as a specific structural type among the unreinforced masonry typology. URM building typologies in ELER tool cover a wide range of masonry construction encountered in Europe, such as rubble stone, adobe, simple stone, massive stone, brick masonry with wooden floors and brick masonry with reinforced concrete floors.

The objective of this paper is to introduce a procedure for the development of displacement based fragility curves for typical stone masonry buildings in Old Quebec City and to present the generated results. It was first necessary to make an inventory of the existing masonry buildings and to include their special structural and material characteristics. At the end, a comparison is made with fragility curves implicit in Hazus and ELER seismic risk assessment tools in order to assess differences and the potential disparities they may exert on damage probability estimates.

2 ANALYTICAL FRAGILITY ANALYSIS FRAMEWORK

Fragility refers to the probability of reaching or exceeding a given damage state defined as a function of earthquake loading. The output of the fragility analysis is a set of fragility curves describing different damage or limit states. Fragility curves can be obtained from empirical, judgmental, analytical, and hybrid approaches [5]. All these methods contain epistemic and aleatory uncertainties in the assessment procedures and use data including: measurement uncertainty related to observations of damage, inconsistency in the quality of available databases and related analyses, variability in the ground motions, uncertainty in experts judgment, statistical uncertainty inherent in the parameter estimates, uncertainty due to simplification of strength and stiffness models of structural materials and components, uncertainties in seismic demand and capacity of structures due to variations of their geometry and material properties, uncertainty in the definition of the damage limit states, etc.

Because of the scarcity of observational damage data in regions of moderate seismicity such as Quebec City and the subjectivity of judgmental damage data, modern risk assessment methodologies adopt analytical development of fragility curves. Analytical methods rely on structural modeling and analytical evaluation of the likelihood for a given building to experience damage by earthquakes of a given intensity and distance, as well as on consideration of related uncertainties.

The derivation process of analytical fragility curves for a particular building or building typology comprises several components: (1) buildings Inventory, (2) damage/limit state model, (3) building capacity model, (4) seismic hazard, (5) seismic demand model, and (6) fragility generation (Figure 1).

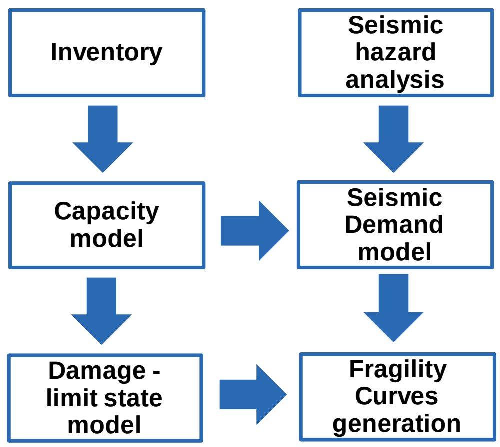

Figure 1: Derivation process of analytical fragility curves.

Fragility curves are given in the form of lognormal fragility distribution that relates the probability of being in or exceeding a given damage state for a given intensity measure (e.g., spectral inelastic displacement demand). The conditional probability of being in or exceeding a particular damage state, DS given the spectral displacement S_d is defined by the function:

$$P\left[DS \mid S_d\right] = \Phi\left[\frac{1}{\beta_{DS}} \ln\left(\frac{S_d}{\overline{S}_{d,DS}}\right)\right]$$

$$\beta_{DS} = \sqrt{CONV(\beta_C, \beta_D)^2 + {\beta_T}^2} \tag{1}$$

where: $\overline{S}_{d,DS}$ is median value of the spectral displacement at which the building reaches the threshold of damage state DS, β_{DS} is standard deviation of the natural logarithm of spectral displacement for damage state DS, and Φ is standard normal cumulative distribution function. β_{DS} describes the total variability of a fragility curve damage state. Three primary sources contribute to the total variability of any given damage state, namely, the variability in the capacity model β_C, the variability in the demand model β_D, and the variability in the threshold of a damage state from the damage model β_T. Since the seismic demand is dependent on the building capacity, a convolution process is required to combine their respective variability [6]. In the case the variability in the seismic demand, β_D, is already modeled in the Probabilistic Seismic Hazard Analysis (PSHA) process, it should be removed from β_{DS} as follows [5],

$$\beta_{DS} = \sqrt{\beta_C^{\,2} + \beta_T^{\,2}} \tag{2}$$

3 INVENTORY OF STONE MASONRY BUILDINGS IN OLD QUEBEC CITY

A detailed inventory has been carried out to characterize the historic stone masonry buildings in Old Quebec City. Besides the field survey, the inventory consisted of review of architectural reports and dissertations, historic documents [7], and archives of the Biliothèque et Archives Nationales du Québec (www.banq.qc.ca).

Figure 2 shows the three most frequent types of stone masonry buildings, selected among the typologies reported by Vallières [7] and retained as representative structural types for the study area. These building types were constructed during the 18th and mid-19th century. The massive façade walls are relatively thick, ranging from 40 to 60 cm, and have regular window and door openings on both sides of the building. The typical story height ranges from 2.75m to 3.35m. Lateral fire walls are of the same thickness as the façade walls. The typical floor is made of wood resting on the façade walls. The massive façade and fire walls provide the buildings' lateral resistance in both directions.

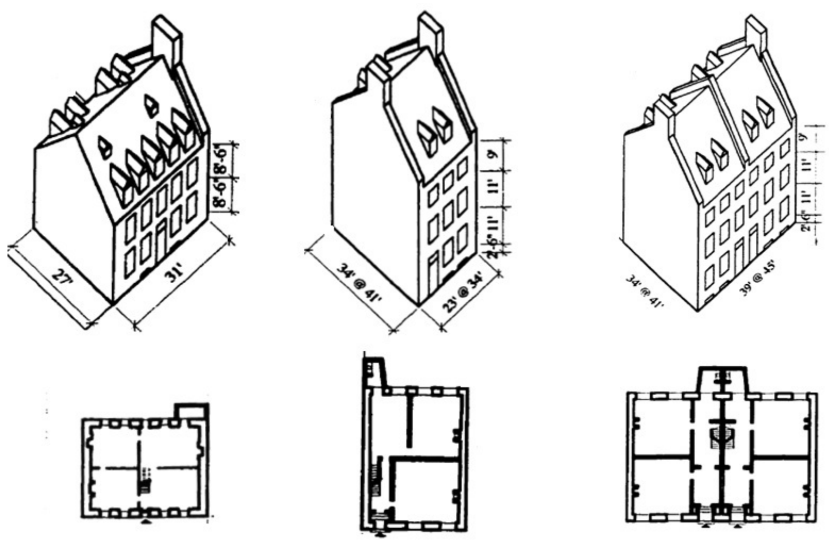

Figure 2: Main stone masonry building typologies in Old Quebec City **[7]**.

4 DISPLACEMENT-BASED DAMAGE MODEL AND FRAGILITY CURVES

The good correlation between the earthquake induced displacement and the extent of structural damage lead to the development of modern performance-based seismic assessment procedures which are based on the evaluation of the structure-specific deformation capacity and earthquake-induced displacement demand.

Recently, simplified displacement-based procedures were proposed for the risk assessment of masonry structures [8] and [9]. The procedure proposed in [9] is adopted in this study. It assumes modeling of the masonry structures by an equivalent single degree of freedom system with effective global parameters (ESDOF). The structural damage state threshold at the effective height of the ESDOF is obtained according to the assumed deformed shape of the structure. A linear shape is assumed for elastic behavior and a soft story deformed shape is assumed for inelastic behavior which is the most common failure mechanism of masonry structures under earthquake loading (Figure 3.a). Damage state drift thresholds for masonry walls are identified from experiments on masonry wall elements.

The displacement at the threshold of each damage state at the effective height of the ESDOF Δ_{DSi} , equivalent to the spectral displacement, and can be evaluated as:

$$\Delta_{DSi} = \theta_{DS1}.k_1.H + (\theta_{DSi} - \theta_{DS1}).k_2.h_s \tag{3}$$

where: H is total height of the building, h_s is height of the first story walls, θ_{DS1} is drift threshold for the first story walls at the elastic limit, θ_{DSi} is the drift threshold for the first story walls at higher damage states, k_1 is the effective height coefficient to convert the multi degree of freedom system into ESDOF, k_2 is the effective height of the first story walls going into the inelastic range when openings are present, k_2 =1.0 when there are no openings.

For a regular distribution of masses and a uniform story height, k_1 is equal to 0.667. When the mass distribution is not regular, what is common in the case of unreinforced stone masonry, the buildings are better represented by a distributed mass corresponding to the mass of the masonry walls plus lumped masses corresponding to the mass at each floor. In this case, k_1 and k_2 have to consider the different mass distributions. The computation of these two factors is explained in details by [9] and the proposed values are given in Table 1.

Damage states drift thresholds are identified on the envelope curve of stone masonry walls as shown in Figure 3.b [10] and [11]. The lateral response of stone masonry walls is strongly nonlinear. As the displacement due to cracking increases, the walls experience both strength and stiffness degradation. The thresholds on the horizontal axis correspond to flexural cracking (θ_{DS1}), shear cracking (θ_{DS2}), maximum shear strength (θ_{DS3}), and ultimate deformation at 20% loss of strength (θ_{DS4}). They are considered as respective thresholds for the slight damage state, moderate damage state, extensive damage state, and complete damage state.

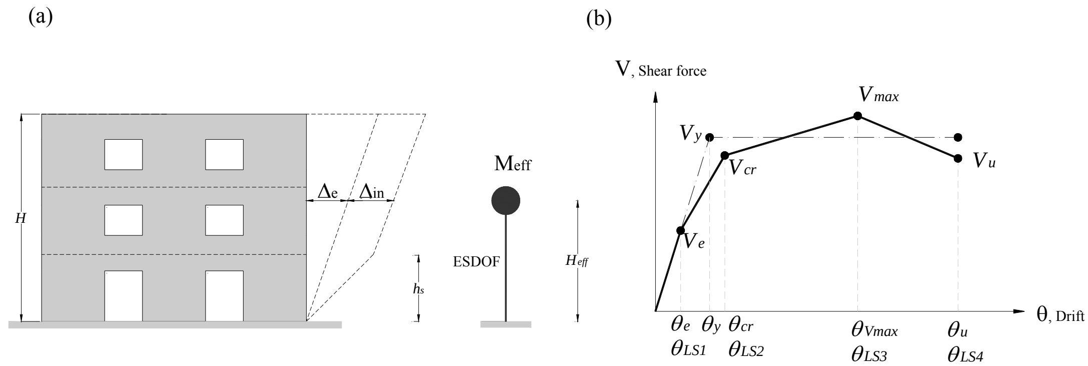

Figure 3: Simplified model for damage limit states (a), and identification of drift limits for masonry walls (b).

Number of stories	k_1	k_2
1	0.79	0.96
2	0.72	0.95
3	0.69	0.92

Table 1: Values of effective height coefficients of the ESDOF for different number of stories [9].

In the context of this study there are no laboratory test results on stone masonry walls representative for URM in the Old Quebec City, therefore damage states drift thresholds were derived from typical literature data on stone masonry wall elements [11];[12];[13]. A Matlab code [14] was used to obtain an empirical cumulative distribution (CDF) of each damage state drift threshold from collected data. The lognormal cumulative distribution was employed to fit the empirical distribution. This parametric probability distribution has the advantage of being fully defined by two statistical parameters that incorporate the central tendency (median) and dispersion (lognormal standard deviation) of the data (Figure 4.a). These values were implemented in Equation 3 as lognormal distributed random variables. The story height value was assumed deterministic as the median height from the inventory (h_s = 3.0m). The respective displacement threshold resulting data were then fitted with lognormal distributions which represent the displacement threshold fragility curves of the ESDOF (Figure 4.b).

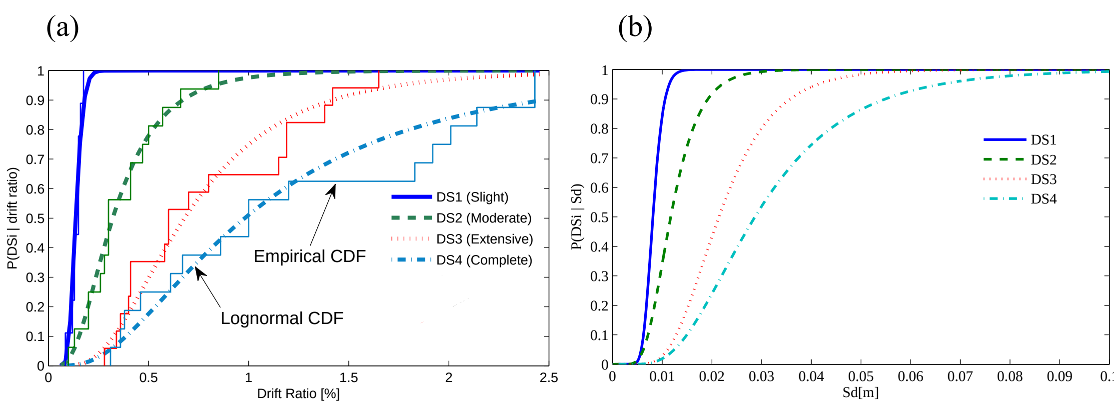

Figure 4: Drift threshold variability (a), and Displacement-based damage threshold fragility curves for two-story stone masonry buildings (b).

Figure 5 illustrates the developed fragility curves for two-story stone masonry buildings. For comparative purposes, the fragility curves for the Hazus pre-code unreinforced masonry buildings (URM) and ELER simple stone low-rise buildings are also presented. For the moderate damage state (DS2), the median displacement threshold $\overline{S}_{d,DS2}$ developed in this study is 0.7 and 3.3 fold of those implicit in Hazus and ELER, respectively. For the complete damage state (DS4), $\overline{S}_{d,DS4}$ developed in this study is 0.3 and 2.4 fold of those implicit in Hazus and ELER, respectively. The lognormal standard deviation of the moderate and complete damage state threshold are $\beta_{T,DS2} = 0.38$ and $\beta_{T,DS4} = 0.50$, respectively. This is in fair agreement with the assumed standard deviation in both Hazus and ELER for all damage states, $\beta_{T,DSi} = 0.4$. This variability can be reduced by conducting laboratory tests on typical stone masonry walls found in Old Quebec City.

One can argue that these curves can not be directly compared because of the different assumptions, information and tools used in the development process. The objective of Figure 5 is rather to show the importance for the development of specific fragility curves that reflect the generic construction characteristics for the considered study area.

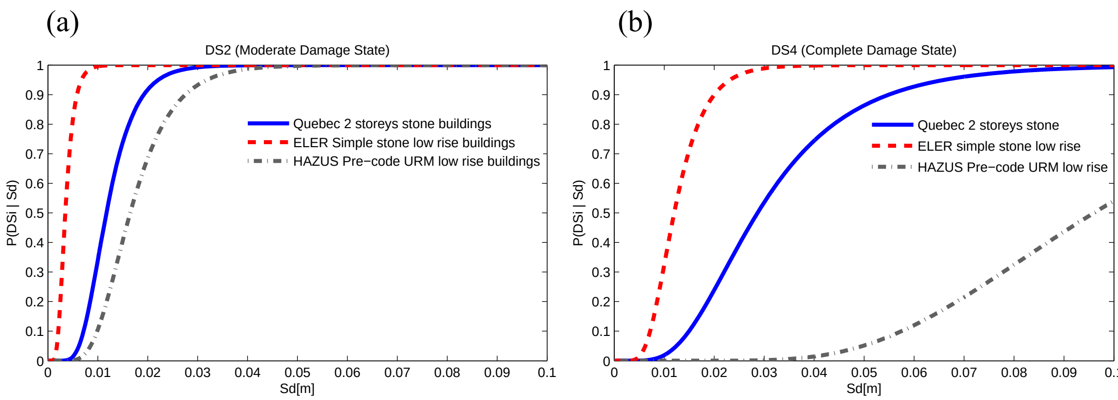

Figure 5: Comparison of fragility curves of Quebec, Hazus and ELER for (a) moderate damage state and (b) complete damage state.

5 CAPACITY MODEL

The three main typologies of existing stone masonry buildings typologies (Figure 2) were used to develop the capacity model. The variation in capacity of stone masonry buildings is relatively high since small modification in geometry or in material properties may result in different seismic resistance. Quebec City stone masonry buildings are mainly constructed from limestone and sometimes sandstone with lime mortar. However, no specific information on material mechanical properties was available. These properties were therefore obtained from the literature data [15], and may introduce significant variability in the developed capacity models.

In order to develop a representative capacity model for a building typology, a simplified mechanical model was used with some modifications [16]. The elastic deformation of the building is approximated by a linear shape up to the point where the shear capacity of the wall is reached, whereas the inelastic deformation is assumed perfectly plastic and concentrated at the first story, which is the typical damage observed in past earthquakes. The effective stiffness of the linear elastic part can be determined using secant stiffness at the capacity, V_y, and is selected such that the bilinear curve is equivalent to the experimental curve using the Energy equivalence criteria [17]. The base shear strength of the building in one direction is assumed to equal the sum of the shear strengths of the first story walls in that direction (Figure 6). Two simple criteria were used to evaluate the strength of the first story walls based on the expected failure mechanism: flexural rocking failure and diagonal cracking failure [17]. Example of the variability in capacity curves due to material uncertainty is shown in Figure 7 which presents five capacity curves corresponding to different masonry strength. More details about the development of capacity curves for the selected typologies can be found in [18].

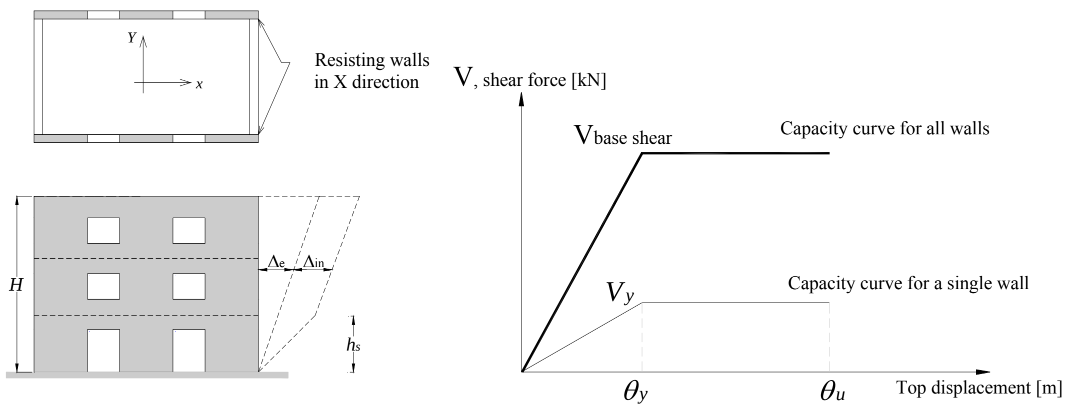

Figure 6: Simplified mechanical model for capacity curve evaluation of stone masonry buildings.

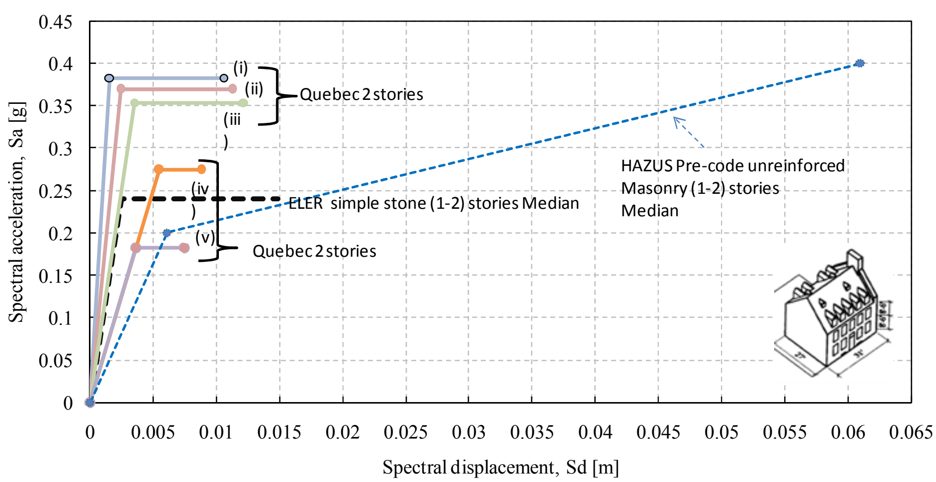

Figure 7: Variability in capacity curves for a Quebec City stone masonry typology and comparison with Hazus and ELER tools respective median capacity curves.

The fitted lognormal distributions for the capacity model parameters, the fundamental period of vibration and the yield acceleration, are shown in Figure 8. The median fundamental period of vibration for 1 to 2 story buildings considered in this study is 0.18sec, with a lognormal standard deviation of 0.34. This value is in agreement with the ELER value (0.19sec), however, it is stiffer than the respective median value implicit in Hazus (0.35sec). The median yield acceleration is 0.30g with 0.26 lognormal standard deviation, which is slightly higher than the corresponding median values implicit in ELER (0.24g) and in Hazus (0.2g) both characterized with lognormal standard deviations of 0.3.

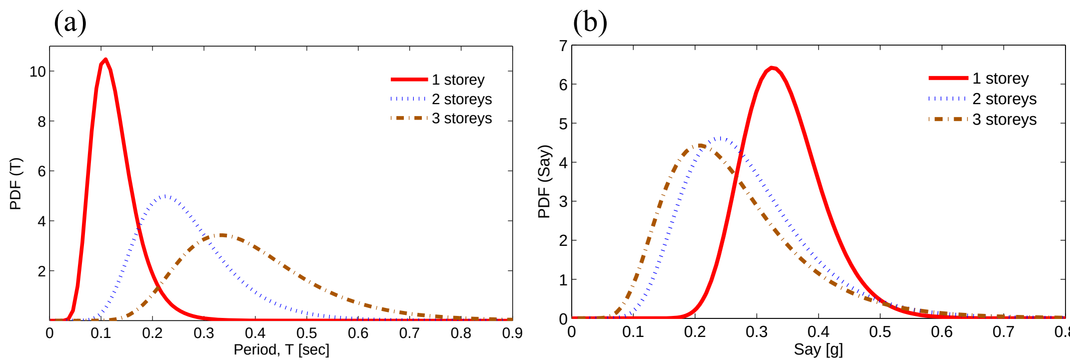

Figure 8: Statistics of the capacity model: fundamental period variation (a) and yield acceleration variation (b).

6 FRAGILITY BASED SEISMIC DAMAGE ASSESSMENT

The displacement based fragility curves with combined variability in capacity and damage state threshold, equation 2, were used for determining the damage state probabilities of two-story stone masonry buildings in Old Quebec City at a specific earthquake median uniform hazard levels with 2% probability of exceedance in 50 years obtained from PSHA [19].

The improved displacement coefficient method (DCM) presented in [20] was used to evaluate the spectral displacement demand which is the input to the displacement based fragility curves. The DCM essentially modifies the linear elastic response of the ESDOF system with 5% damping by multiplication with a series of coefficients to generate an estimate of the inelastic displacement demand S_d .

$$\begin{aligned} S_d &= C_1.C_2.S_a(T_e).\frac{T_e^2}{4.\pi^2}.g \\ C_1 &= 1+\frac{R-1}{a.T_e^2} \\ C_2 &= 1+\frac{1}{800}\left[\frac{R-1}{T_e}\right]^2 \\ R &= \frac{S_a(T_e)}{S_{ay}} \end{aligned} \tag{4}$$

where, C_1 is modification parameter which relates the expected maximum displacement of an inelastic ESDOF system with elastic-plastic hysteresis properties to the displacement calculated from the linear elastic spectral response, a is related to the type of local NEHRP soil classification (a=130 for soil class B - rock), C_2 accounts for the effects of pinched hysteresis shape, stiffness degradation, and strength deterioration on the maximum displacement response, $S_a(T_e)$ is the spectral acceleration at the effective fundamental period of the system coming from the capacity curve, and S_{ay} is the yield acceleration of the system. The median T_e and S_{ay} of the two-story stone masonry buildings were obtained from the capacity model as 0.25sec and 0.24g, respectively. The corresponding spectral acceleration $S_a(T_e)$ with 2% probability of exceedance in 50 years is 0.49g, and spectral displacement S_d is 0.01m.

The final damage state probabilities are shown in Figure 9 together with respective damage probabilities obtained from fragility curves defined in Hazus and ELER. For the given spectral displacement demand, discrete damage state probabilities are evaluated as the difference of the cumulative probabilities of reaching or exceeding successive damage states. The damage estimation obtained using Hazus shows highest probability of occurring to no damage and to slight damage, ELER yields highest probabilities to extensive and complete damage, whereas damage estimates generated by this study and for the same intensity measure (S_d=0.01m) indicate that slight to moderate damage will be the most probable damage experienced by the stone masonry buildings.

This comparative example shows the importance of the development of specific fragility curves that reflect the generic construction characteristics for the considered study area for seismic risk assessment and emphasizes the need of critical use of existing risk assessment tools and the obtained results.

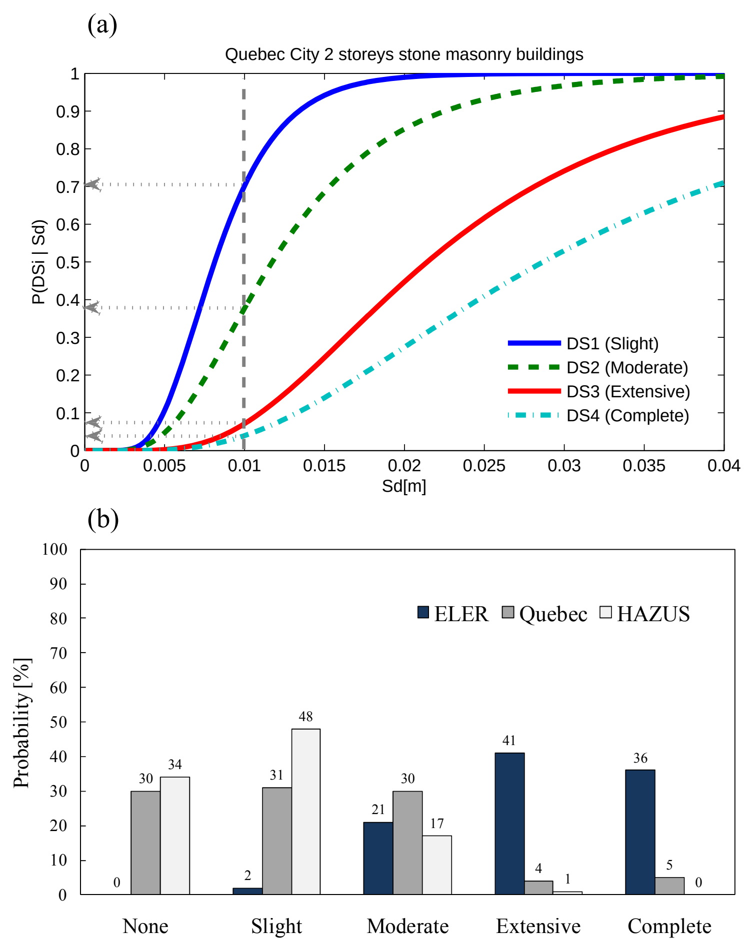

Figure 9: Damage state probabilities for Old Quebec City two-story stone masonry buildings (a), compared with respective damage states computed with fragility curves implicit in Hazus and ELER (b).

7 CONCLUSIONS

The procedure for analytical displacement based fragility analysis of stone masonry buildings in Old Quebec City is presented. The first step consisted of an inventory of existing buildings in the study area and characterization of representative typologies of stone masonry buildings. These typologies were utilized to develop a building capacity model using a simplified mechanical model with linear elastic and perfectly plastic domains which proved particularly effective for carrying out analyses of uncertainties with significantly reduced computational time.

A simplified displacement based procedure was used to develop damage state fragility curves based on drift limits of stone masonry walls which were assigned based on literature data. It is expected that using drift limits obtained from laboratory testing of stone masonry walls representative of those existing in Old Quebec City would help to reduce the uncertainties in the damage prediction. A comparison of the developed fragility curves is made with their corresponding curves in existing regional seismic risk assessment tools Hazus and ELER. Significant differences have been observed between fragility curves defined by the three methodologies. These differences were replicated in comparatively significant disparities among the estimates of the probabilities of different damages states to be experienced by stone masonry buildings in the Old Quebec City for the same seismic hazard with probability of 2% exceedance in 50 years.

REFERENCES

[1] Tomaževic.M, *Earthquake-Resistant Design of Masonry Buildings*, *Innovation in Structures and Construction, Vol. 1*, Editors: Elnashai, A.S. & Dowling, P.J., Imperial College Press, London, 268 pages, 1999.

[2] Chidiac, S.E., Foo, S., and Cheung M.S., Seismic guidelines for stone-masonry components and structures. *Proceedings of the Int. Conference on the Seismic Performance of Traditional Buildings*, Turkey, 13 pages, 2000.

[3] FEMA-NIBS, HAZUS-MH MR4: Multi-hazard Loss Estimation Methodology Earthquake Model Technical manual. *Federal Emergency Management Agency (FEMA), National Institute of Building Science (NIBS)*, Washington, D.C, 712 pages, 2003.

[4] Demircioglu, M. B., Erdik, M., Hancilar, U., Sesetyan, K., Tuzun,C., Yenidogan, C., and Zulfikar, A. C., Technical Manual – Earthquake Loss Estimation Routine ELER-v2.0. *Bogazici University, Department of Earthquake Engineering, Istanbul*, 133 pages, 2009.

[5] Calvi GM, Pinho R, Magenes G, Bommer JJ, Restrepo-Velez LF, Crowley H., The development of seismic vulnerability assessment methodologies for variable geographical scales over the past 30 years. *ISET Journal of Earthquake Engineering Technology*, **43**(3), 75–104, 2006.

[6] Kircher, C. A., A. A. Nassar, et al., Development of Building Damage Functions for Earthquake Loss Estimation. *Earthquake Spectra,* **13**(4), 663-682, 1997.

[7] Vallieres, A., Processus de transformation typologique du bâti résidentiel dans l'arrondissement historique du Vieux-Québec. *Mémoire de maîtrise. Université Laval, École d'architecture*, 221 pages, 1999.

[8] Calvi, G.M., A displacement-based approach for vulnerability evaluation of classes of buildings. *Journal of Earthquake Engineering*, **3**(3), 411-438, 1999.

[9] Restrepo-Vélez, L.F., A Simplified Mechanics-Based Procedure for the Seismic Risk Assessment of Unreinforced Masonry Buildings. *Individual Study, European School for Advanced Studies in Reduction of Seismic Risk (ROSE School)*, Pavia, Italy, 2003.

[10] V. Bosiljkov, A.W. Page, V. Bokan-Bosiljkov and R. Zarnic, Evaluation of the seismic performance of brick masonry walls. *Structural Control and Health Monitoring,* **17**(1), 100–118, 2010.

[11] M.Tomaževic, P.Weiss., Displacement capacity of masonry buildings as a basis for the assessment of behavior factor: and experimental study. *Bulletin of earthquake engineering,* **8**(6), 1267-1294, 2010.

[12] Tomaževič. M, Lutman. M., Heritage Masonry Buildings in Urban Settlements and the Requirements of Eurocodes: Experience of Slovenia. *International Journal of Architectural Heritage*, **1**, 108-130, 2007.

[13] Vasconcelos, G., Experimental investigations on the mechanics of stone masonry: Characterization of granites and behaviour of ancient masonry shear walls. *PhD Thesis, University of Minho, Guimarães*, Portugal, 2005.

[14] Matlab User's Guide, www. mathworks.com.

[15] Mazzon, N., Influence of Grout Injection on the Dynamic Behaviour of Stone Masonry Buildings. *Doctoral dissertation, University of Padova*, Italy, 306 pages, 2010.

[16] Lang, K.. Seismic vulnerability of existing buildings. *Swiss Federal Institute of Technology, ETHZ, Zurich*, Switzerland, 200 pages, 2002.

[17] Magenes, G. & Calvi, G.M., In-Plane Seismic Response of Brick Masonry Walls. *Earthquake Engineering and Structural Dynamics*, **26**(11), 1091-1112, 1997.

[18] Abo-El-Ezz.A, Nollet. M.J, Nastev.M., Characterization of historic stone masonry buildings in old Quebec City for seismic risk assessment. *Submitted to the Canadian Society of Civil Engineers Annual Conference*, Ottawa, June, 2011.

[19] Adams J, Halchuk S., Fourth generation seismic hazard maps of Canada: Values for over 650 Canadian localities intended for the 2005 National Building Code of Canada. *Geological Survey of Canada Open File no. 4459*, 155 pages, 2003.

[20] FEMA 440: Improvement of nonlinear static seismic analysis procedures. *Federal Emergency Management Agency, Applied Technology Council, Washington D.C.*, USA, Rep. No. 440, 2005.